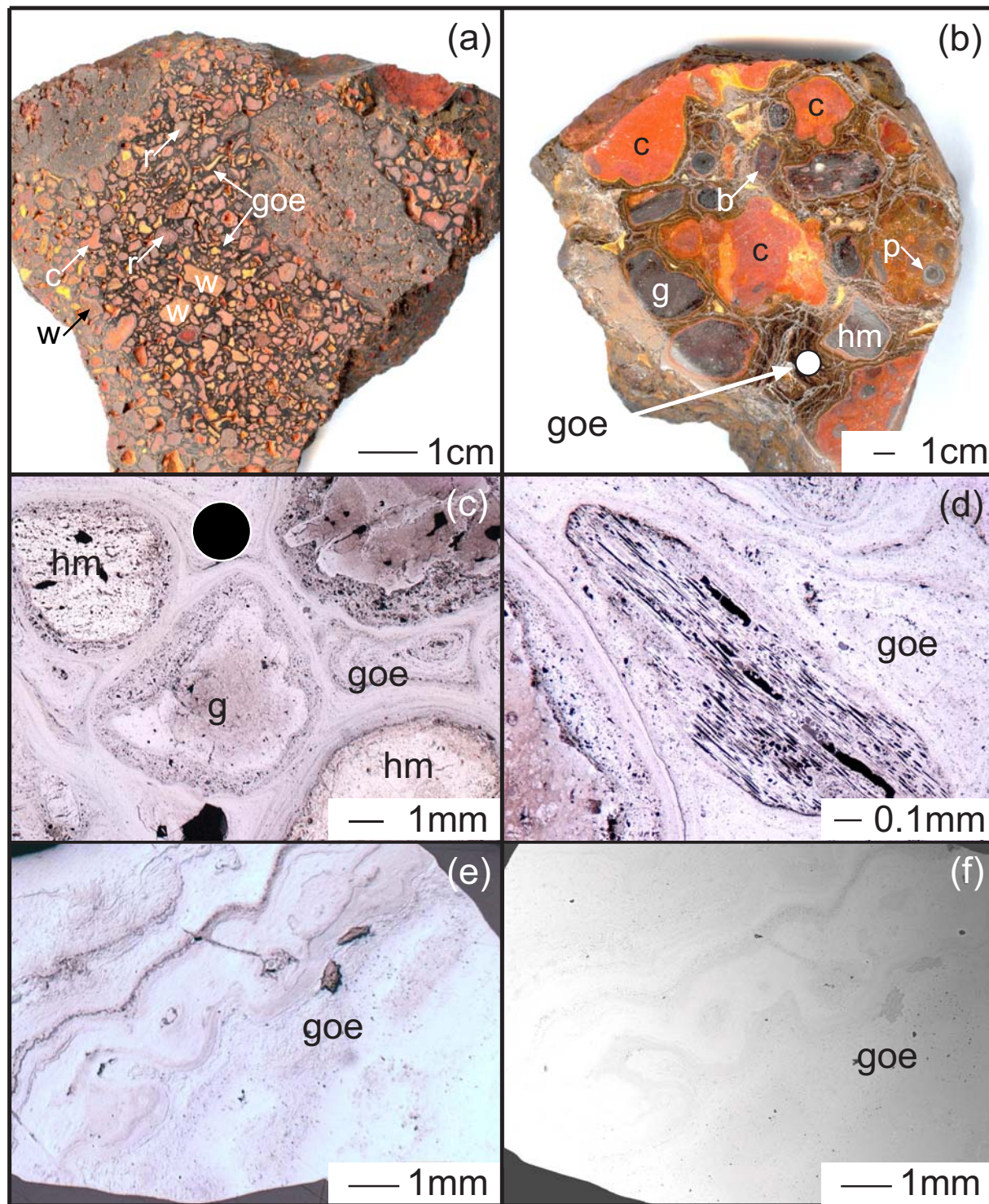


Figure A1. Scanned images of polished blocks, and reflected light and electron photomicrographs from the Yandi Channel Iron Deposit.

- (a) A polished block of typical Yandi ore composed of ferruginized wood (w) fragments (yellow to light orange), ferruginized clay pods (c), and ferruginized rock fragments (r). The detrital material is cemented by a crystalline, finely banded (botryoidal) vitreous dark brown goethite cement (goe). Goethite growth bands are continuous around several detrital fragments and throughout the whole sample, indicating the goethite cement dated in this study precipitated after the deposition of the detrital material. This late-stage goethite cement composes ~40 – 50 volume % of the Yandi ore.
- (b) A polished block of typical Yandi ore composed of ferruginized clays or clay-rich sediments (c), fragments of ferruginized banded iron-formation (b), fragments of goethite (g) and hematite (h), and iron-rich pisoids (p) all cemented by vitreous botryoidal brown goethite (goe). The continuity of the goethite cement around several detrital fragments and throughout the whole sample once again indicates ferruginization of the channel sediments after deposition. Light brown-red and yellow goethite reaction rims surround some detrital fragments, possibly indicating metasomatic replacement reactions that occurred in the channel. Late-stage clays (c) fill cavities in the goethite cement. The filled white circle indicates the location of goethite cement recovered by drill core for (U-Th)/He dating.
- (c) Reflected light photomicrograph of Yandi ore showing fragments of detrital hematite (h) and goethite (g) enveloped by goethite growth bands (forming pisoids) and cemented by late-stage botryoidal goethite (goe). Note the reaction rims of goethite surrounding the detrital fragments and the continuity of the late-stage goethite cement around several pisoids, as described above. The filled black circle indicates the approximate location of the goethite dated in this study.
- (d) Reflected light photomicrograph showing a detrital wood fragment pseudomorphically replaced by finely crystalline goethite and cemented by late-stage vitreous goethite (goe). The black areas are voids between the goethitised wood cell walls.
- (e) Reflected light photomicrograph of a grain of goethite (goe) recovered from the cement of Yandi ore and similar to those dated in this study. The goethite is visually pure and has a finely banded botryoidal texture.
- (f) A backscatter electron photomicrograph (15kV, 10mm) reveals that the grain illustrated in (e) is composed entirely of goethite (goe), with a relatively homogeneous chemical composition, and devoid of detrital phases.



CAPTIONS

Tables A2-1 to A2-3. Stepped heating data files for YAN02-01-A (A2-1), YAN02-01-D1 (A2-2), and YAN02-01-D2 (A2-3). b.d. is below detection.

Figure A2-1. ${}^3\text{He}$ Arrhenius plots for (a) YAN02-01-A, (b) YAN02-01-D1 and (c) YAN02-01-D2. Diamonds are values calculated from release fractions of proton-induced ${}^3\text{He}$ according to Fechtig and Kalbitzer (1966). The dashed lines are the least squares regressions through the high retentivity domains (HRD) of each sample (Shuster et al., 2005). The solid curves are the two-domain models used to construct the curves shown in **Fig. A2-2**, calculated following the procedures and assumptions described in Shuster et al. (2005). For reference, the dotted lines are the diffusion parameters of the low retentivity domains (LRD) and f_V denotes the volume fraction of each domain used to construct the two-domain models.

Figure A2-2. Goethite ratio evolution diagrams for (a) YAN02-01-A, (b) YAN02-01-D1 and (c) YAN02-01-D2. Shown are measured isotope ratios for each release step, R_{step} ($R = {}^4\text{He}/{}^3\text{He}$), normalized to the bulk ratio R_{bulk} plotted vs. the cumulative ${}^3\text{He}$ release fraction, $\Sigma F {}^3\text{He}$. Five two-domain diffusion models are shown for each sample with deficit gas fractions (as per cent) for the HRD indicated in the legend. Assumptions in the models are the same as those discussed in Shuster et al. (2005). The LRDs were assumed to contain no ${}^4\text{He}$, since the LRD diffusion kinetics for each shown in **Fig. A2-1** predicts essentially no radiogenic ${}^4\text{He}$ retention over geologic time. QR denotes quantitative ${}^4\text{He}$ retention in the HRD. Error bars (1σ) are specified

by vertical line through each point. Data scatter and uncertainty is largely a function of ${}^4\text{He}$ blank corrections. From these diagrams, we conclude the following deficit gas fractions apply to the HRD of YAN02-01-A, YAN02-01-D1, and YAN02-01-D2, respectively: $10 \pm 5\%$, $10 \pm 5\%$, and $20 \pm 10\%$. These, in conjunction with the LRD volume fractions, can be used to correct the (U-Th)/He ages for diffusive ${}^4\text{He}$ loss according to Shuster et al., (2005).

Appendix 2 References

- Fechtig, H., and Kalbitzer, S., 1966, The diffusion of argon in potassium-bearing solids, in Schaeffer, O.A., and Zahringer, J., eds., Potassium-Argon Dating: Heidelberg, Springer, p. 68-106.
- Shuster, D.L., Vasconcelos, P.M., Heim, J.A., and Farley, K.A., 2005, Weathering geochronology by (U-Th)/He dating of goethite: Geochimica et Cosmochimica Acta, v. 69, p. 659-673.

Table A2-1: YAN02-01-A

Step	T (°C)	time (hr)	${}^3\text{He}$ (atoms/ 10^6)	$R_{\text{step}}/R_{\text{bulk}}^*$	(+/-)
1	50	5	2.15	b.d.	b.d.
2	65	5	6.61	b.d.	b.d.
3	80	4	10.24	b.d.	b.d.
4	100	2	15.85	0.05	0.02
5	125	2	38.87	0.18	0.04
6	150	1	43.81	0.30	0.03
7	175	1	78.84	0.43	0.02
8	200	1	128.64	0.72	0.01
9	200	1	99.55	0.89	0.02
10	200	1	106.78	0.95	0.02
11	190	1	53.27	0.98	0.03
12	180	2	46.59	0.98	0.05
13	170	3	31.07	0.88	0.08
14	160	3	11.57	0.93	0.14
15	150	4	5.56	0.95	0.22
16	140	5	2.87	0.99	0.28
17	180	3	73.27	0.99	0.02
18	205	2	285.88	0.96	0.01
19	210	1	182.91	0.97	0.01
20	215	1	224.95	0.91	0.01
21	220	1	217.56	0.89	0.01
22	225	1	145.16	0.94	0.01
23	230	1	62.17	1.02	0.02
24			346.10	1.80	
Total			2220.28		

 $*R = {}^4\text{He}/{}^3\text{He}$, $R_{\text{bulk}} = 107$

Table A2-2: YAN02-01-D1

Step	T (°C)	time (hr)	${}^3\text{He}$ (atoms/ 10^6)	$R_{\text{step}}/R_{\text{bulk}}^*$	(+/-)
1	50	5	3.01	b.d	b.d
2	65	5	7.50	b.d	b.d
3	80	4	16.23	b.d	b.d
4	100	2	22.97	b.d	b.d
5	125	2	57.15	0.07	0.03
6	150	1	65.27	0.22	0.03
7	175	1	109.41	0.39	0.02
8	200	1	157.77	0.66	0.02
9	200	1	101.25	0.90	0.03
10	200	1	105.64	0.95	0.03
11	190	1	66.32	0.97	0.03
12	180	2	54.97	0.97	0.05
13	170	3	36.17	0.92	0.08
14	160	3	16.10	0.99	0.09
15	150	4	8.40	0.93	0.14
16	140	5	3.84	0.90	0.20
17	175	4	71.68	0.99	0.04
18	195	3	197.30	0.98	0.01
19	205	2	270.45	0.96	0.00
20	210	1	205.92	1.01	0.01
21	215	1	251.15	1.06	0.01
22	220	1	211.46	1.08	0.01
23	225	1	172.48	1.08	0.01
24	230	1	103.80	1.13	0.02
25	235	1	36.25	1.13	0.06
26	240	1	9.72	1.18	0.17
27	245	1	6.91	1.13	0.21
28	250	1	5.12	1.43	0.27
29	275	1	13.95	1.43	0.13
30	300	1	30.55	1.12	0.07
31	325	1	30.76	1.13	0.07
32	350	1	35.66	1.20	0.06
33	400	1	76.00	1.13	0.03
34	550	0.5	99.16	1.13	0.02
35	550	1	6.85	1.32	0.22
36	550	2	3.96	1.05	0.27
37			8.27	24.47	
Total			2679.40		

 $*R = {}^4\text{He}/{}^3\text{He}$, $R_{\text{bulk}} = 144$

Table A2-3: Yan02-01-D2

Step	T (°C)	time (hr)	${}^3\text{He}$ (atoms/ 10^6)	$R_{\text{step}}/R_{\text{bulk}}^*$	(+/-)
1	50	5	4.39	b.d	b.d
2	65	5	11.43	b.d	b.d
3	80	4	20.32	b.d	b.d
4	100	2	29.68	0.03	0.01
5	125	2	66.60	0.22	0.05
6	150	1	77.25	0.29	0.05
7	175	1	137.86	0.45	0.04
8	200	1	279.57	0.76	0.02
9	200	1	255.56	0.91	0.02
10	200	1	252.04	0.93	0.02
11	190	1	107.03	0.96	0.04
12	180	2	80.57	0.95	0.06
13	170	3	43.89	0.96	0.09
14	160	3	16.60	0.97	0.15
15	150	4	8.45	0.93	0.22
16	140	5	4.06	0.96	0.29
17	175	4	82.34	0.99	0.04
18	195	3	311.90	0.98	0.01
19	205	2	317.43	1.03	0.01
20	210	1	140.81	1.13	0.04
21	215	1	126.08	1.15	0.05
22	220	1	104.26	1.18	0.05
23	225	1	73.06	1.15	0.10
24	230	1	43.11	1.24	0.11
25	235	1	24.66	1.04	0.17
26	240	1	8.57	1.33	0.30
27	245	1	4.99	1.23	0.37
28	250	2	13.43	1.01	0.21
29	275	1	20.87	0.94	0.15
30	300	1	35.35	1.17	0.11
31	325	1	38.84	1.12	0.12
32	350	1	42.20	1.13	0.11
33	400	1	77.75	1.12	0.07
34	550	0.5	129.44	1.14	0.04
35	550	1	13.53	1.05	0.24
36	550	2	6.75	1.17	0.35
37	550	3	4.03	1.10	0.40
38			11.22	22.18	
Total			3025.94		

 $*R = {}^4\text{He}/{}^3\text{He}$, $R_{\text{bulk}} = 69$

